

A Highly Oriented Cubic Phase Formed by Lipids under Shear

Annela M. Seddon,^{*,†,§} Gudrun Lotze,[‡] Tomás S. Plivelic,[⊥] and Adam M. Squires^{*,‡}

[†]H.H. Wills Physics Laboratory, Tyndall Avenue, University of Bristol, Bristol BS8 1TL, United Kingdom

[§]Bristol Centre for Functional Nanomaterials, Nanoscience and Quantum Information Building, Tyndall Avenue, University of Bristol, Bristol BS8 1FD, United Kingdom

[‡]School of Chemistry, Whiteknights Campus, University of Reading, Reading RG6 6AD, United Kingdom

[⊥]MAX IV Laboratoriet, Lund University, 22100 Lund, Sweden

S Supporting Information

ABSTRACT: We demonstrate the formation of a macroscopically oriented inverse bicontinuous cubic (Q_{II}) lipid phase from a sponge (L_3) phase by controlled hydration during shear flow. The L_3 phase was the monoolein/butanediol/water system; the addition of water reduces the butanediol concentration, inducing the formation of a diamond (Q_{II}^D) cubic phase, which is oriented by the shear flow. The phenomenon was reproduced in both capillary and Couette geometries, indicating that this represents a robust general route for the production of highly aligned bulk Q_{II} samples, with applications in nanomaterial templating and protein research.

Inverse bicontinuous cubic (Q_{II}) phases are nanostructured materials formed by lipid self-assembly. In this paper, we demonstrate a method for the production of a macroscopically oriented sample of a Q_{II} phase.

Biological amphiphiles such as lipids are known to be capable of forming 3-D self-assembled nanostructures known as Q_{II} phases.¹ Three such cubic phases have been reported, known as the Diamond (Q_{II}^D), Gyroid (Q_{II}^G), and Primitive (Q_{II}^P), illustrated in Figure 1. In each case, the lipid molecules form an intricately curved fluid bilayer, on either side of which lie two interpenetrating continuous networks of water channels. The structures of Q_{II} phases possess a number of remarkable features that have significant potential for nanotechnological applications. They contain water channels of the order of 2–5 nm in diameter, whose size is extremely uniform throughout the sample, the dimensions of which may be tuned by controlling the temperature (in excess water) or the lipid/water ratio (below excess water).² The structure also provides an extremely efficient way of packing a very large contiguous surface area into a small volume.³ Such properties make these, and similar structurally analogous materials, promising candidates in applications where they may be templated for size-selective molecular sieves or catalysts⁴ or for electronic applications.⁵ They have also shown success as a matrix for the crystallization of membrane proteins⁶ and as a host for siRNA.⁷ Moreover, given the biological origin of the amphiphiles, and the similarity of the bilayer environment within the Q_{II} phase to a cell membrane, they have much more widespread potential in protein research.⁸ However, until now research has

almost exclusively employed bulk samples containing billions of randomly oriented domains.⁹ In general, single crystal or oriented monodomain materials can have vastly different properties as compared with their polydomain or powder-like analogues. For example, internal domain boundaries can potentially affect transport, mechanical and optical properties.¹⁰ Specifically for bicontinuous cubic phases, the internal domain boundaries are known to affect phase transition kinetics.¹¹ Macroscopically oriented materials also yield information that cannot be obtained from powder-like samples, especially when studied using diffraction techniques such as small-angle X-ray scattering (SAXS), which is a major technique for structural studies of cubic phases.^{12,13} For example, the mechanism of interconversion of lyotropic phases cannot be determined unambiguously using powder-like samples.¹³ There are many other instances of research where X-ray scattering analysis yields more information as a result of sample orientation, for example, on a surface¹⁴ or of fibers oriented by flow.¹⁵

It would therefore be advantageous if there were a method to produce macroscopically oriented cubic phases of biological amphiphiles. The work we present here demonstrates such a method, based on the transformation of a disordered precursor “sponge” phase into a cubic phase under controlled hydration during shear flow.

The sponge or L_3 phase can be considered as a disordered cubic phase which still displays a bicontinuous network of water channels separated by a lipid bilayer.¹⁷ It possesses short-range order; however, it is disordered over longer length scales. Amphiphiles which spontaneously form cubic phases are often seen to form L_3 phases in the presence of additives which cause a relaxation of the curvature of the cubic phase, leading to this disordered structure.^{18,19} Structurally analogous systems formed by surfactant/brine mixtures have been well characterized in the past.^{16,20} The L_3 phase formed by lipids has been documented in detail in the case of the lipid 1-monoolein (MO) in the presence of additives commonly found in membrane protein crystallization;¹⁸ indeed, it is postulated that in-cubo crystallization may occur via an L_3 intermediate. In contrast to the Q_{II} phases which are extremely stiff with typical shear modulus of the order of hundreds of kilopascals,²¹ the L_3 phase has a much lower viscosity, and flows as a liquid.²²

Received: June 9, 2011

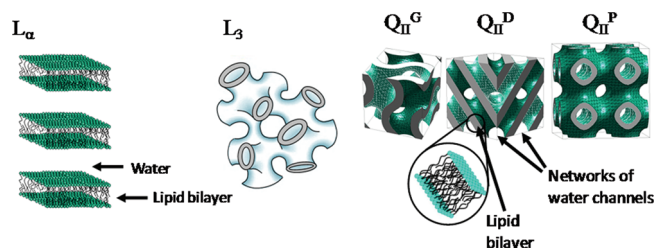


Figure 1. The bicontinuous phases formed by monoolein. From left to right, the L_3 , or sponge, phase (image adapted from ref 16); the Q_{II}^G (gyroid), the Q_{II}^D (diamond), and the Q_{II}^P (primitive) inverse bicontinuous cubic phases.

In this work, the L_3 phase formed by MO, in the presence of 1,4-butanediol and water, is transformed to a Q_{II}^D phase by reducing the concentration of 1,4-butanediol. This process involves controlled dilution of the sample. Furthermore, by performing this dilution under shear flow, both in a flow cell and a Couette cell, a macroscopically oriented cubic phase was formed. The phase diagram of the MO/butanediol/water system¹⁸ shows that for a fixed w/w ratio of MO to “solvent” (i.e., the mixture of butanediol and water), three distinct phases are formed depending on the butanediol/water ratio. Below 25% (v/v) butanediol, the $Pn3m$ phase is observed. From 25% to ~45% butanediol, the sample exists in the L_3 phase. At butanediol concentrations >45% of the total volume of solvent, a fluid lamellar phase is observed. This can be rationalized by consideration of the effect of an amphiphilic additive such as butanediol on the interfacial curvature of the lipid membrane. Interactions of the butanediol with both the polar/apolar interface and the apolar region of the bilayer causes swelling of the aqueous channels and relaxation of the bilayers such that the cubic phase becomes disordered and phases with flatter interfaces such as the L_3 or the fluid lamellar phase emerge. Here, we have started with a butanediol concentration of 40%; by adding water, we have effectively lowered the concentration of butanediol causing the sample to move into the Q_{II}^D phase—removal of butanediol effectively increases the interfacial curvature of the membrane. By performing this dilution under shear, as the cubic phase forms, it macroscopically orientates leading to the highly ordered material shown in our work.

A 60:40 (v/v) solution of water/1,4-butanediol was prepared and mixed with MO (Rylo, received as a gift from Danisco) in a 60:40 (w/w) solvent/MO ratio. The sample underwent 2 freeze thaw cycles to form an optically isotropic viscous liquid. Data was collected at I711 at Max-lab in a custom built syringe pump driven flow cell using 1.5 mm internal diameter fluorinated ethylene propylene (FEP) tubing connected to a 1.5 mm diameter thin walled borosilicate glass X-ray capillary. The beam size at the sample was 0.35×0.35 mm (full width at half-maximum, fwhm). Data were also collected at the ID02 high brilliance beamline at the ESRF using a Haake RS300 rheometer fitted with an X-ray transparent polyimide Couette cell (inner diameter 20 mm, outer diameter 22 mm, height 40 mm, 1 mm gap). The L_3 phase was loaded into either the flow cell or Couette cell and a static SAXS pattern was measured, confirming the presence of the L_3 phase. For the flow cell, water was loaded into the FEP tubing and separated from the L_3 phase by an air gap of approximately $5 \mu\text{L}$. The sample was flowed back and forth at a volume flow rate of $10 \mu\text{L s}^{-1}$ and a displaced volume of $50 \mu\text{L}$

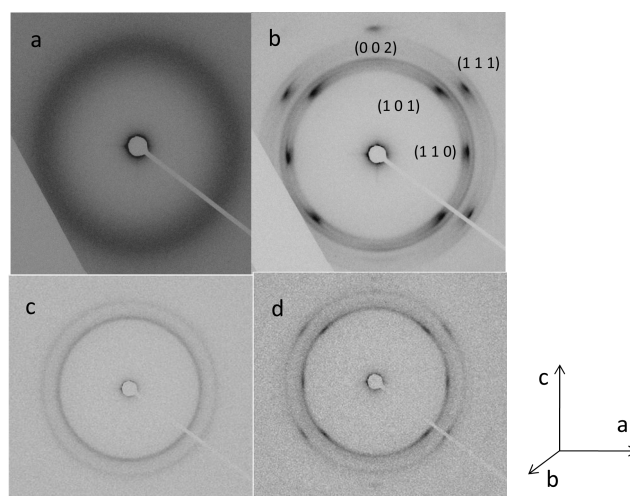


Figure 2. Data collected from the flow cell: (a) The L_3 phase formed prior to flow; (b) the oriented Q_{II}^D phase formed after oscillatory flow has been applied. The cubic phase shows cylindrical symmetry about the (001) (c) axis; (c) data collection in first 30 s reveals that cubic phase is formed (d) which subsequently aligns. In the axis system shown, the X-ray beam passes in the (b) direction, while (c) represents the capillary axis and thus the direction of flow.

(approximately 36 mm linear displacement). In the case of the Couette cell, a known volume of water was added manually between the inner and outer walls of the Couette. Large amplitude oscillatory shear was applied at a frequency of 1 Hz at a strain amplitude of $\gamma = 1000$. Images were recorded over a range of time scales with an exposure time of either 10 or 60 s (Max-lab) or 0.1–1 s (ESRF). The images were analyzed using a custom written macro in ImageJ. Integrated data are given in the Supporting Information.

Figure 2 shows the data collected in the flow cell. Figure 2a illustrates that the MO/butanediol/water sample is in an L_3 phase prior to dilution, or to the application of shear flow as observed previously.¹⁸ As water was added to the sample under oscillatory shear or flow, butanediol was effectively diluted leading to an increased interfacial curvature and the formation of a highly oriented Q_{II}^D phase shown in Figure 2b. The scattering pattern is consistent with an oriented cubic phase arranged with the [010] axis parallel to the flow direction, which is vertical as shown in the image. The diffraction pattern is rotationally averaged about this direction due to the symmetry of the flow apparatus. Data collection in first 30 s reveals that a cubic phase is formed which subsequently aligns. This is shown in Figure 2c,d. We estimate from the experiments carried out in the Couette cell that we moved from a butanediol ratio of 40% (v/v) to 15% (v/v) which would be sufficient to drive a phase transition from L_3 to Q_{II}^D in agreement with previous observations.¹⁸

While the observed lattice parameters of the L_3 and Q_{II}^D samples are smaller than those observed previously,¹⁸ the lattice parameter of the Q_{II}^D is still swollen by 37.5 \AA (from $a = 100 \text{ \AA}$ ^{23,24} previously seen for MO in water to 137.5 \AA , decreasing to 125.5 \AA over the course of the alignment) above what would be seen for a Q_{II}^D formed by MO and water and confirms that the addition of 1,4-butanediol causes the sample to swell. The data taken in the Couette cell follows the same pattern (data not shown).

Shear was halted and images were recorded to examine the stability of the oriented cubic phase. During a 10 min period, no

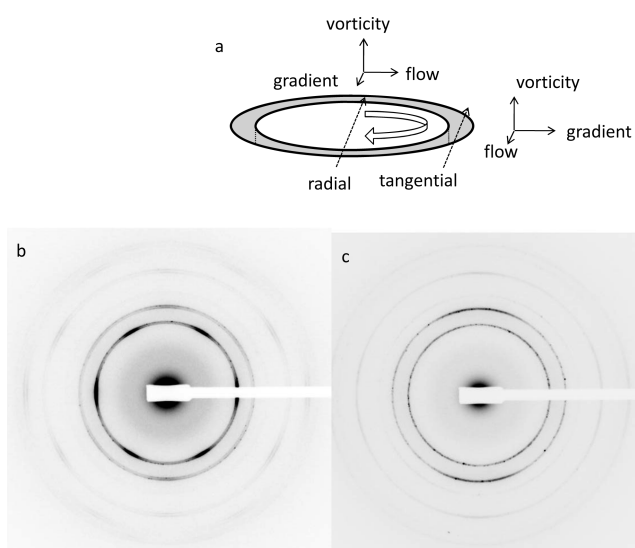


Figure 3. Data collected from the Couette cell: (a) schematic showing the direction of flow of the sample relative to the X-ray beam path; (b) SAXS pattern of an aligned Q_{II}^D phase taken radial to the beam path; (c) the aligned Q_{II}^D phase viewed tangential to the beam path.

change was observed in the sample, indicating that, at least over this time scale, the sample was stable in an aligned configuration.

Data were collected in a Couette cell to examine the alignment of the sample both radial and tangential to the X-ray beam. These patterns are shown in Figure 3. Two scattering patterns were obtained, with the beam passing radially (through the center of the Couette cell cylinders) and tangentially (in between the cylinders, on one side). In the radial geometry, the beam passes in the shear gradient direction, and the scattering pattern shows the vorticity-flow plane (illustrated schematically in Figure 3a). The pattern is the superposition of scattering from the front and back of the cylinder, leading to the closely spaced double reflections that can be seen in Figure 3b. The pattern again shows a high degree of orientation. In this case, there is a pronounced 6-fold rotational symmetry about the beam direction, possibly suggesting that the beam is passing along a body diagonal ($\langle 111 \rangle$ axis) of the cubic phase. The tangential scattering pattern shown in Figure 3c shows a much lower degree of orientation, suggesting some level of rotational disorder about the flow direction.

Overall, the flow cell appears to provide more oriented samples, although, in general, Couette cells provide better defined shear flow regimes. Interestingly, the two methods provide cubic phases with different orientations.

Previous work on sheared type I (“normal”) cubic phases²⁵ showed that when a cubic phase formed by a nonionic surfactant subjected to shear in a Couette cell, “melting” of the cubic phase into what was postulated to be the L_3 phase occurred. Upon cessation of shear, the cubic phase reformed; however, now it displayed a preferred orientation. Single crystals of a Q_{II}^G phase have also been observed previously in surfactant and block copolymer systems; however, these have been grown epitaxially from corresponding lamellar or hexagonal phases.^{26–28}

We suggest that the ability to form an aligned cubic phase of this nature opens up the possibility of improved nanostructured templating applications, enhanced *in cubo* crystallization of proteins and increased structural information on globular and membrane proteins incorporated within the cubic matrix.^{6,29}

Starting from an L_3 phase has practical advantages, namely, that its low viscosity compared to the Q_{II}^D phase allows facile loading of the sample into a flow cell. In conclusion, we have shown that by starting from a disordered precursor phase in the form of the L_3 phase formed by MO and butanediol, it is possible to produce an aligned macroscopically oriented cubic phase of lipid.

■ ASSOCIATED CONTENT

S Supporting Information. Integrated SAXS data for Figures 2a–d and 3b,c. This material is available free of charge via the Internet at <http://pubs.acs.org>.

■ AUTHOR INFORMATION

Corresponding Authors

annela.seddon@bristol.ac.uk; a.m.squires@reading.ac.uk

■ ACKNOWLEDGMENT

G.L. is supported by funding from the University of Reading and the Diamond Light Source. We thank the ESRF and Max-lab for the provision of beamtime.

■ REFERENCES

- (1) Luzzati, V.; Delacroix, H.; Gulik, A.; Gulik-Krzywicki, T.; Mariani, P.; Vargas, R. *Lipid Polymorphism and Membrane Properties*; Academic Press: San Diego, CA, 1997; Vol. 44, pp3–24.
- (2) Squires, A. M.; Seddon, J. M.; Templer, R. H.; Templer, R. H.; Leatherbarrow, R. *Biophysical Chemistry: Membranes and Proteins*; The Royal Society of Chemistry: Cambridge, U.K., 2002; p 177–190.
- (3) Shearman, G. C.; Ces, O.; Templer, R. H.; Seddon, J. M. *J. Phys.: Condens. Matter* **2006**, *18*, S1105–S1108.
- (4) Holyst, R. *Nat. Mater.* **2005**, *4*, 584–584.
- (5) Wang, D. H.; Luo, H. M.; Kou, R.; Gil, M. P.; Xiao, S. G.; Golub, V. O.; Yang, Z. Z.; Brinker, C. J.; Lu, Y. F. *Angew. Chem., Int. Ed.* **2004**, *43*, 6169–6173.
- (6) Caffrey, M. *Ann. Rev. Biophys.* **2009**, *38*, 29–51.
- (7) Leal, C. I.; Bouxsein, N. F.; Ewert, K. K.; Safinya, C. R. *J. Am. Chem. Soc.* **2011**, *132*, 16841.
- (8) Bilewicz, R.; Rowinski, P.; Rogalska, E. *Bioelectrochemistry* **2005**, *66*, 3–8.
- (9) Rittman, M.; Frischherz, M.; Burgmann, F.; Hartley, P. G.; Squires, A. *Soft Matter* **2010**, *6*, 4058–4061.
- (10) Biggins, J. S.; Warner, M.; Bhattacharya, K. *Phys. Rev. Lett.* **2009**, *103*, 037802.
- (11) Conn, C. E.; Ces, O.; Mulet, X.; Finet, S.; Winter, R.; Seddon, J. M.; Templer, R. H. *Phys. Rev. Lett.* **2006**, *96*, 108012.
- (12) Squires, A. M.; Templer, R. H.; Seddon, J. M.; Woenckhaus, J.; Winter, R.; Finet, S.; Theyencheri, N. *Langmuir* **2002**, *18*, 7384–7392.
- (13) Squires, A. M.; Templer, R. H.; Seddon, J. M.; Woenckhaus, J.; Winter, R.; Narayanan, T.; Finet, S. *Phys. Rev. E* **2005**, *72*, 011502.
- (14) Caracciolo, G.; Amenitsch, H.; Sadun, C.; Caminiti, R. *Chem. Phys. Lett.* **2005**, *405*, 252–257.
- (15) Squires, A. M.; Devlin, G. L.; Gras, S. L.; Tickler, A. K.; MacPhee, C. E.; Dobson, C. M. *J. Am. Chem. Soc.* **2006**, *128*, 11738–11739.
- (16) Porcar, L.; Hamilton, W. A.; Butler, P. D.; Warr, G. G. *Phys. Rev. Lett.* **2004**, *93*, 198301.
- (17) Porte, G. *Curr. Opin. Colloid Interface Sci.* **1996**, *1*, 345–349.
- (18) Cherezov, V.; Clogston, J.; Papiz, M. Z.; Caffrey, M. *J. Mol. Biol.* **2006**, *357*, 1605–1618.
- (19) Wadsten-Hindrichsen, P.; Bender, J.; Unga, J.; Engstrom, S. *J. Colloid Interface Sci.* **2007**, *315*, 701–713.

- (20) Hamilton, W. A.; Porcar, L.; Butler, P. D.; Warr, G. G. *J. Chem. Phys.* **2002**, *116*, 8533–8546.
- (21) Mezzenga, R.; Meyer, C.; Servais, C.; Romoscanu, A. I.; Sagalowicz, L.; Hayward, R. C. *Langmuir* **2005**, *21*, 3322–3333.
- (22) Munoz, J.; Alfaro, M. C. *Grasas Aceites* **2000**, *51*, 6–25.
- (23) Briggs, J.; Chung, H.; Caffrey, M. J. *Phys. II* **1996**, *6*, 723.
- (24) Qiu, H.; Caffrey, M. *Biomaterials* **2000**, *21*, 223–234.
- (25) Olsson, U.; Mortensen, K. J. *Phys. II* **1995**, *5*, 789–801.
- (26) Rancon, Y.; Charvolin, J. J. *Phys. (Paris)* **1987**, *48*, 1067–1073.
- (27) Rancon, Y.; Charvolin, J. J. *Phys. Chem.* **1988**, *92*, 2646–2651.
- (28) Schulz, M. F.; Bates, F. S.; Almdal, K.; Mortensen, K. *Phys. Rev. Lett.* **1994**, *73*, 86–89.
- (29) Zabara, A.; Amar-Yuli, I.; Mezzenga, R. *Langmuir* **2011**, *27*, 6418–6425.